Pressure-Dependent Gas Heat Transport in a Spherical Pore

Jeffrey R. Wolf and William C. Strieder
Dept. of Chemical Engineering, University of Notre Dame, Notre Dame, IN 46556

A mean free path gas kinetic theory is used to model the conductive heat transport of a gas within a void volume enclosed in a Fourier solid. A variational upper bound principle is derived for a void of arbitrary shape and applied to obtain a rigorous upper bound equation for the void gas conductivity in a spherical void. The variational void gas conductivity equation is exact in both the large and small Knudsen number (Kn) limits and provides a means to determine the accuracy of the reciprocal additivity interpolation formula as applied to thermal conductivity rather than diffusive mass transfer (maximum error 6% at $Kn = 0.5$ and $\alpha = 1$). Temperature jump will occur even at atmospheric pressures and higher for sufficiently small thermal accommodation coefficients ($\alpha < 0.1$). Experimental void gas heat conductivities vs. pressure data for H_2, He, Ne, N_2, CO_2, and F12 in a polyurethane foam are compared with theoretical mean free path void gas conductivity vs. inverse Knudsen number curves drawn for various α. Estimates of the thermal accommodation coefficients for the gas- polyurethane surface exhibit a maximum with increasing molecular mass of the gas molecules, which qualitatively agrees with the predictions of Baule's classical theory. Results also point to a rather sharp shift of the S curve to higher pressures with decreasing thermal accommodation.

Introduction

The thermal design of low temperature production (Hands, 1986) and storage systems (Kramer et al., 1984) requires the use of special thermal insulations and a knowledge of their thermal conductivities. Multilayer insulation (Timmerhaus 1975), consisting of alternating layers of highly reflecting material and a low conducting spacer under high vacuum, provide the best cryogenic insulation with conductivities normal to the layers as low as 10^{-5} W/mK, but are costly (Barron, 1985), difficult to apply to complicated shapes, have a high lateral conductivity, and experience structural deterioration (Tien and Streton, 1987). Powder or fibrous insulation, which realize some of the benefits of multiple shields without the expense and structural complexities, but with a one- or two-order reduction in thermal effectiveness, are more commonly found in commercial applications. Foams (Boetes and Hoogendorn, 1987) with the advantage of low density and high compressive strength, are also widely used in low temperature insulation.

Correspondence concerning this article should be addressed to W. C. Strieder.
Current address of J. R. Wolf: Ethyl Corp., Process Development Center, P.O. Box 341, Baton Rough, LA 70821.

For efficient cryogenic insulation the void gas within the insulator space is maintained at lower pressures between the continuum and Knudsen plateaus. Under these conditions, a modest decrease in pressure significantly lowers the void gas conductivity (Kaganer, 1969). The Knudsen conductivity limit and the entire S curve decrease with pressure from bulk to Knudsen conductivity both feature their dependence on the pore structure and the gas-solid surface interaction. Gas conductivities in each of the various cryogenic insulations mentioned in the first paragraph will have different S curves and Knudsen plateaus (Zheng and Strieder, 1994). Further, any prediction of a shift of the S curve to higher pressures with change in the thermal energy surface accommodation or solid dispersion geometry would be of great interest. Thus, expressions for the low-pressure transition region gas conductivity within the cells of a foam or the void regions of powder and fibrous insulation would be useful.

The low-pressure gas conduction in cryogenic insulation requires a kinetic theory of gases for an analysis. Kennard (1938), using an approximate temperature jump method, derived a void gas conductivity λ_g, which can be written in the form of

a series addition of the higher pressure continuum λ_o and low-pressure Knudsen λ_{Kn} gas thermal conductivities:

$$\lambda_g^{-1}(\text{series}) = \lambda_o^{-1} + \lambda_{Kn}^{-1} \tag{1}$$

with the Knudsen conductivity given by:

$$\lambda_{Kn} = \left[\frac{\alpha}{2-\alpha}\right]\left[\frac{(\gamma+1)k}{2(\gamma-1)}\psi\right]\delta. \tag{2}$$

The heat capacity ratio γ is c_p/c_v, and k is the Boltzmann constant. The effusive mass driving force $\psi[=P(2\pi mkT)^{-1/2}]$, a constant across the cryogenic insulation, is customarily evaluated at an average pressure $\overline{P}$ and temperature $\overline{T}$. Values (Springer, 1971) of the thermal accommodation coefficient α can run from 0.017 for He on clean Tungsten at 30°C, 0.29 for H_2 on glass at 25°C, up to 1.0 for H_2 on glass at −170°C. Kennard's derivation contains a number of limiting assumptions, is done only for the slip region near the continuum pressure limit, and assumes an unrealistic model void geometry, heat flux between two infinite parallel plates. Equations 1 and 2 have been used by many to estimate void gas transport in polymeric foams (Kaganer, 1969; Pleasant, 1986), as well as granular systems (Wakao and Vortmeyer, 1971; Cunningham and Tien, 1977) and fibrous insulation (Kaganer, 1969). In such cases, the plate separation δ in Eq. 2 is usually replaced, ad hoc, by a characteristic length parameter of the pore structure.

In this article, we will develop a kinetic theory for low-pressure gas thermal conductivity within closed voids, based on the mean free path model of gaseous transport (Ho and Strieder, 1981), appropriate for cellular foam insulation. A variational upper bound principle for any enclosure geometry that includes both the Fourier thermal profiles in the surrounding solid and kinetic theory gaseous heat transport in the void is derived. A spherical void of radius a is a sufficiently straightforward geometry to illustrate the value of the variational method and gives an analytical gas conductivity equation in terms of the thermal accommodation coefficient α, the Knudsen number ($Kn = \ell/2a$), and the continuum conductivity λ_o. The equations generate the familiar S curves with pressure for various α, along with some interesting and useful quantitative information. Temperature jump can occur at the void-solid interface, and should be included in the boundary conditions, even at atmospheric pressures for sufficiently small thermal accommodation coefficients ($\alpha < 0.1$). In general, the reciprocal additivity of Eq. 1 is a reasonably good approximation in thermal conductive transport, but does give a measurable error (Figure 1) for higher accommodation coefficients and at gas pressures near the center of the transition region. Experimental gas conductivities vs. pressure S curves, measured by Harper and El Sahrigi (1984) for H_2, He, Ne, N_2, CO_2, and Freon 12 in a polyurethane foam, lie within the α range predicted by the model (Figure 4), and exhibit some of the expected trends in α with molecular structure.

Fundamental Equations

One of the simplext kinetic theory models for gaseous transport, the elementary mean free path model of gas kinetic theory

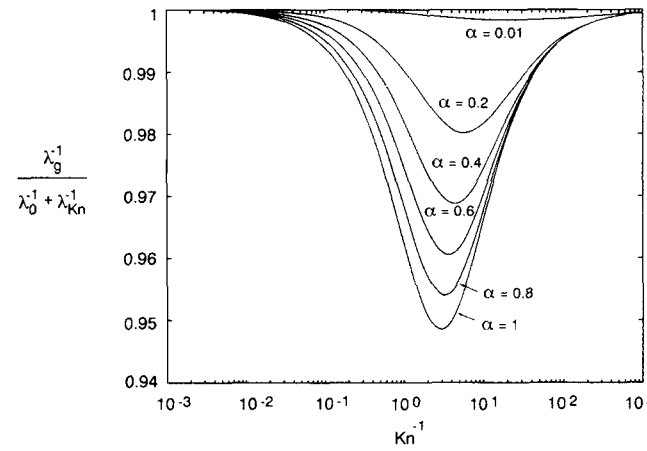

Figure 1. Ratio of the series additivity interpolation formula estimate of the transition region void gas conductivity to the variational mean free path conductivity of Eq. 44 vs. the inverse Knudsen number Kn^{-1} $(=2a/\ell)$ for thermal accommodation coefficients α.

The transition λ_g, bulk λ_o, and Knudsen void gas conductivities λ_{Kn} all come from Eq. 44 for a spherical void.

(Pollard and Present,1948; Ho and Strieder, 1980; 1981), assumes gas molecules leave a molecular collision isotropically, and the fraction of molecules that are ejected from a small void volume after molecular collision within that volume, and travel a distance ρ or greater before collision with another molecule, is $\exp[-\rho/\ell]$, where ℓ is the mean free path for molecule-molecule collisions. If in addition explicit boundaries are present (Pollard and Present, 1948; Present, 1958; Ho and Strieder, 1980) which reflect according to the laws of diffusive reflection, the thermal motion of "tagged" molecules in a pure gas within a void space of average pore diameter $2a$ from Knudsen conduction ($\ell \gg 2a$) to continuum transport ($\ell \ll 2a$) and arbitrary void size and shape can be treated.

In order to describe the steady-state heat transport within the void of a void-solid system, variables are introduced defining the energy transport of the gas streams. $E_i(\underline{r})$ represents the energy flux incident to a unit area on the void-solid interface located at $\underline{r}$, due to the gas molecules arriving at the surface. $E_r(\underline{r})$ is the total energy flux of gas molecules leaving the unit area element of void wall at the surface point $\underline{r}$, and $E_w(\underline{r})$ is the energy flux a gas stream departing the same element would carry, if it were issuing from a gas in thermal equilibrium at the solid surface temperature T_w located at $\underline{r}$. Also, $E_\phi(\underline{r})$ is defined to be the total energy of the gas molecules that undergo molecular collision within a unit void volume at $\underline{r}$ and are isotropically emitted from that volume per unit time. To write energy balances in the void and on the surface in terms of E_r and E_ϕ, the probabilities associated with each molecular free path are introduced following the work of Clausing (1929), Chambré (1960), Strieder (1971), and others. These probabilities have been used successfully in the past to calculate mass diffusion rates for a wide variety of model pore structures. A molecular free path begins with a collision, the molecule then traces out a straight line trajectory, and finally the free path ends with a subsequent collision. As the beginning and ending collisions occur with either a surface or another gas molecule, four types of free path probabilities are possible.

$K_1(\underline{r}, \underline{r}')d^2\underline{r}$ is the probability that a molecule leaving a collision with a pore wall at $\underline{r}'$ will experience its next collision within the wall surface element $d^2\underline{r}$ located at $\underline{r}$.

$K_2(\underline{r}, \underline{r}')d^2\underline{r}$ is the probability that a molecular free path which begins with a molecular collision in a unit void volume located at $\underline{r}'$ will end with a pore wall surface collision within $d^2\underline{r}$ at $\underline{r}$.

$K_3(\underline{r}, \underline{r}')d^3\underline{r}$ is the probability that a molecule just leaving a collision within a unit element of pore wall at $\underline{r}'$ will have its next collision with another molecule in the void volume $d^3\underline{r}$ located at $\underline{r}$.

$K_4(\underline{r}, \underline{r}')d^3\underline{r}$ is the probability that a molecule which begins a free path with a molecular collision in a unit void volume located at $\underline{r}'$ will next collide with another molecule in the void volume $d^3\underline{r}$ located at $\underline{r}$.

Since cosine law diffusive scattering at the pore walls and self diffusion in the gas are assumed, the free path probabilities can be calculated from elementary kinetic theory (Pollard and Present, 1948; Strieder, 1971) with

$$K_1(\underline{r},\underline{r}') = -[\underline{\eta}(\underline{r})\cdot\underline{\rho}][\underline{\eta}(\underline{r}')\cdot\underline{\rho}](\pi\rho^4)^{-1}\exp(-\rho\ell^{-1}) \quad (3)$$

$$K_2(\underline{r},\underline{r}') = [\underline{\eta}(\underline{r})\cdot\underline{\rho}](4\pi\rho^3)^{-1}\exp(-\rho\ell^{-1}) \quad (4)$$

$$K_3(\underline{r},\underline{r}') = -[\underline{\eta}(\underline{r}')\cdot\underline{\rho}](\ell\pi\rho^3)^{-1}\exp(-\rho\ell^{-1}) \quad (5)$$

$$K_4(\underline{r},\underline{r}') = (4\pi\ell\rho^2)^{-1}\exp(-\rho\ell^{-1}) \quad (6)$$

where $\underline{\rho} = \underline{r}' - \underline{r}$, and $\underline{\eta}(\underline{r})$ is a unit normal located at the point $\underline{r}$ pointing away from the solid into the void. Note that any of the K probabilities is zero when the straight-line molecular free path between $\underline{r}$ and $\underline{r}'$ is blocked by intervening solid material. While all the K functions are positive, only K_1 and K_4 remain unchanged with $\underline{r}$ and $\underline{r}'$ are interchanged:

$$K_1(\underline{r},\underline{r}') = K_1(\underline{r}',\underline{r}) \quad (7a)$$

$$K_4(\underline{r},\underline{r}') = K_4(\underline{r}',\underline{r}) \quad (7b)$$

while K_2 and K_3 follow the rule:

$$K_3(\underline{r},\underline{r}') = K_2(\underline{r}',\underline{r})\chi^2 \quad (7c)$$

with:

$$\chi^2 = (4/\ell). \quad (8)$$

Suppose now that a large solid slab (Figure 2) of total volume V consists of an enclosed void volume V_ϕ and a solid-phase volume V_s. The ends of the slab are coincident with planes located at $x=0$ and $x=L$, and $\underline{i}$ is a unit vector pointing across the slab in the positive x-direction. The interfacial area Σ between the two phases makes up the void-solid interface. The energy flux of gas molecules issuing from a gas in equilibrium at the surface temperature (Shidlovsky, 1967) is:

$$E_w = \frac{1}{2}\frac{\gamma+1}{\gamma-1}k\psi T. \quad (9)$$

As in Eq. 2 the effusive mass driving force ψ and heat capacity ratio $\gamma(=c_p/c_v)$ are constant in the void space of a low-pressure

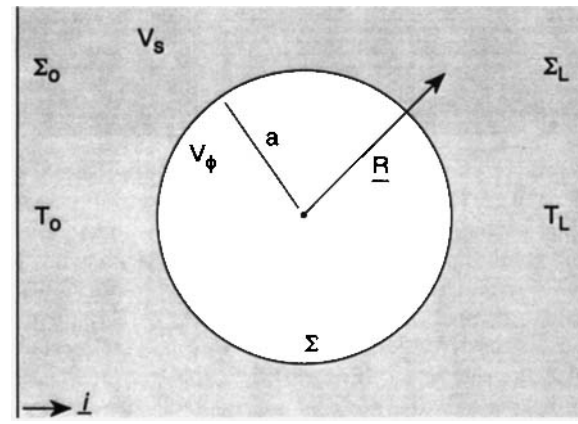

Figure 2. Spherical void volume.

insulation. The accommodation coefficient, which is a measure of the fraction of energy that is transferred from the gas upon collision to the solid is defined in terms of E_r, E_w, and E_i (Shidlovsky, 1967) as:

$$\alpha = \frac{E_r - E_i}{E_w - E_i} \quad (10)$$

Relating the incident energy flux E_i with the temperature T and the departing energy flux E_r by combining Eqs. 9 and 10 gives:

$$E_r = \alpha\frac{1}{2}\frac{\gamma+1}{\gamma-1}k\psi T + (1-\alpha)E_i \quad (\underline{r} \text{ on } \Sigma) \quad (11)$$

The various E functions are determined from local steady-state heat balances using the K probabilities (Eqs. 3-6).

Of the departing molecules with energy flux $E_r(\underline{r}')d^2\underline{r}'$ leaving $d^2\underline{r}'$ on Σ at $\underline{r}'$, only the fraction $K_1(\underline{r}, \underline{r}')E_r(\underline{r}')d^2\underline{r}'$ will arrive at a unit area at $\underline{r}$ on Σ without collision; and of the molecules leaving the volume element $d^3\underline{r}'$ located at $\underline{r}'$ after collision in that volume with the associated molecular energy outflow $E_\phi(\underline{r}')d^3\underline{r}'$ per unit time, only the fraction $K_2(\underline{r}, \underline{r}')E_\phi(\underline{r}')d^3\underline{r}'$ will arrive directly onto a unit area at $\underline{r}$ on Σ without an intervening collision. Then the total incident energy flux of gas molecules at $\underline{r}$ on Σ is:

$$E_i(\underline{r}) = \int_\Sigma K_1(\underline{r},\underline{r}')E_r(\underline{r}')d^2\underline{r}' + \int_{V_\phi} K_2(\underline{r},\underline{r}')E_\phi(\underline{r}')d^3\underline{r}' \quad (\underline{r} \text{ on } \Sigma). \quad (12)$$

When the incident flux E_i from Eq. 11 is substituted into Eq. 12, and E_r is subtracted from both sides, an integral equation in terms of E_r, E_ϕ, and T is obtained:

$$\alpha(1-\alpha)^{-1}[E_r(\underline{r}) - CT(\underline{r})] = \int_\Sigma K_1(\underline{r},\underline{r}')E_r(\underline{r}')d^2\underline{r}' - E_r(\underline{r}) + \int_{V_\phi} K_2(\underline{r},\underline{r}')E_\phi(\underline{r}')d^3\underline{r}' \quad (\underline{r} \text{ on } \Sigma) \quad (13)$$

where

$$C=\frac{1}{2}\frac{\gamma+1}{\gamma-1}k\psi=\frac{\gamma+1}{\gamma-1}k\frac{n\bar{v}}{8} \tag{14}$$

the product of the particle density n and mean thermal speed $\bar{v}$, as well as C itself can be considered as a constant. A similar energy balance can be written for molecules undergoing molecular collision in a unit volume of void space V_ϕ at any point $\underline{r}$. Of the molecular energy flux $E_r(\underline{r}')d^2\underline{r}'$ from molecules leaving $d^2\underline{r}$ on Σ, only the fraction $K_3(\underline{r},\underline{r}')E_r(\underline{r}')d^2\underline{r}'$ will trace a single free path to the unit void volume located at $\underline{r}$ and make the next collision in that volume. Of the energy outflow per unit time $E_\phi(\underline{r}')d^3\underline{r}'$ from molecules leaving $d^3\underline{r}'$ after experiencing a molecular collision in that void volume element, only the fraction $K_4(\underline{r},\underline{r}')E_\phi(\underline{r}')d^3\underline{r}'$ will travel a straight line and arrive at the unit void volume at $\underline{r}$ and undergo a molecular collision. Then a steady-state balance of the molecular energy from those molecules arriving and colliding in the unit void volume is:

$$E_\phi(\underline{r})=\int_\Sigma K_3(\underline{r},\underline{r}')E_r(\underline{r}')d^2\underline{r}'+\int_{V_\phi}K_4(\underline{r},\underline{r}')E_\phi(\underline{r}')d^3\underline{r}' \quad (\underline{r}\text{ in }V_\phi) \tag{15}$$

The steady-state energy balance within the solid V_s is given by Fourier's law:

$$\nabla\cdot[\lambda_s\nabla T(\underline{r})]=0 \quad (\underline{r}\text{ in }V_s) \tag{16}$$

with a solid conductivity λ_s, and the local solid temperature $T(\underline{r})$. The thermal boundary condition equating the net energy flux from the surface Σ at $\underline{r}$ to the normal flux from the solid is:

$$-\lambda_s\underline{\eta}\cdot\nabla T(\underline{r})=E_r(\underline{r})-E_i(\underline{r}) \quad (\underline{r}\text{ on }\Sigma) \tag{17}$$

where $\underline{\eta}$ points away from the solid. In terms of E_r and T from Eq. 11:

$$\lambda_s\underline{\eta}\cdot\nabla T(\underline{r})=\frac{\alpha}{1-\alpha}[E_r(\underline{r})-CT(\underline{r})] \quad (\underline{r}\text{ on }\Sigma). \tag{18}$$

Finally, Eqs. 13, 15, 16, and 18 together with the bed and boundary conditions that:

$$T(\underline{r})=\begin{cases}T_o & (x=0)\\ T_L & (x=L)\end{cases} \tag{19}$$

are in principle sufficient to solve for E_r, E_ϕ, and T exactly, but in practice outright solutions are difficult.

In the equilibrium limit of no heat transport, when T_o-T_L is set to zero, the heat transport balances of Eqs. 13 and 15 are simplified. Strieder (1971) has proven the following integral equations always relate the K probabilities:

$$1=\int_\Sigma K_1(\underline{r},\underline{r}')d^2\underline{r}'+\chi^2\int_{V_o}K_2(\underline{r},\underline{r}')d^3\underline{r}' \quad (\underline{r}\text{ on }\Sigma) \tag{20}$$

and

$$1=\frac{1}{\chi^2}\int_\Sigma K_3(\underline{r},\underline{r}')d^2\underline{r}'+\int_{V_o}K_4(\underline{r},\underline{r}')d^3\underline{r}' \quad (\underline{r}\text{ in }V_\phi) \tag{21}$$

where χ^2 is given by Eq. 8. Note, the symmetry conditions of Eqs. 7a, 7b, and 7c on the K free path probability functions were used to obtain the final forms of Eqs. 20 and 21. Equation 20 is the probabilistic statement that a molecule leaving the pore wall surface Σ at $\underline{r}$ must go directly to another surface or void volume before experiencing another collision. Equation 21 states in probabilities that a free path, which begins with a molecular collision in the void, must end either on a surface or with another molecular collision. These geometrical relations Eqs. 20 and 21, together with Eqs. 9, 15, and 17 require an equilibrium constant temperature T_o in the solid:

$$E_r(\underline{r})=E_w(\underline{r})=CT_o \tag{22}$$

and with Eqs. 11, 12, and 13:

$$E_\phi(\underline{r})=\chi^2E_r(\underline{r})=\chi^2CT_o \tag{23}$$

Equations 20-23 will be used in deriving the variational principle and as conditions for the energy flux trial functions.

Variational Formulation

A variational upper bound on the net heat flux $\underline{Q}$, averaged perpendicular to the x-axis over any total cross section of the slab will be derived in this section for arbitrary void geometry. For steady state the net average heat flux $\underline{Q}$ across both the planar surfaces Σ_o and Σ_L located at $x=0$ and $x=L$ is the same. The dot product of $\underline{Q}$ with $C(T_o-T_L)L^{-1}\underline{i}$ can be written in terms of a surface integration over Σ_o and Σ_L as:

$$-\underline{Q}\cdot\underline{\beta}=\frac{1}{V}\int_{\Sigma_o+\Sigma_l}CT(\underline{r})\lambda_s\underline{\eta}\cdot\nabla T(\underline{r})d^2\underline{r} \tag{24}$$

where $\underline{\eta}$ points away from the slab, the boundary condition (Eq. 19) has been used and:

$$\underline{\beta}=C(T_L-T_o)L^{-1}\underline{i}=C\underline{\theta}. \tag{25}$$

The upper bound on the heat flux is based on the variational functional:

$$\begin{aligned}V\Lambda\{E_r^*,E_\phi^*,T^*\}=&\chi^2C\int_{V_s}d^3\underline{r}\lambda_s[\nabla T^*(\underline{r})]^2\\&+\chi^2\frac{\alpha}{1-\alpha}\int_\Sigma d^2\underline{r}[E_r^*(\underline{r})-CT^*(\underline{r})]^2\\&+\frac{\chi^2}{2}\int_\Sigma d^2\underline{r}\int_\Sigma d^2\underline{r}'K_1(\underline{r},\underline{r}')[E_r^*(\underline{r}')-E_r^*(\underline{r})]^2\\&+\int_\Sigma d^2\underline{r}\int_{V_o}d^3\underline{r}'K_2(\underline{r},\underline{r}')[E_\phi^*(\underline{r}')-\chi^2E_r^*(\underline{r})]^2\\&+\frac{1}{2}\int_{V_o}d^3\underline{r}\int_{V_o}d^3\underline{r}'K_4(\underline{r},\underline{r}')[E_\phi^*(\underline{r}')-E_\phi^*(\underline{r})]^2\end{aligned} \tag{26}$$

where the trial temperature T^* must be continuous, piecewise continuously differentiable in V_s, and satisfy the bed end boundary conditions:

$$T^*(\underline{r}) = \begin{cases} T_o & (x=0) \\ T_L & (x=L) \end{cases} \tag{27}$$

As the free path jump probabilities K_1, K_2, and K_4 by Eqs. 3, 4, and 6 are always positive or zero, the quadratic form (Eq. 26) is positive.

To establish the variational upper bound, trial functions for E_r^*, E_ϕ^*, and T^* are substituted into Eq. 26 in the form of the exact solutions (E_r, E_ϕ and T) plus the variation (δE_r, δE_ϕ, and δT). Such a substitution will generate from Λ three parts, a zeroth-order $\Lambda\{E_r, E_\phi, T\}$, a first-order $\delta\Lambda$, and a positive second-order term $\delta^2\Lambda$ in the variation. Collecting all first-order terms in δ from Eq. 26, using the symmetry conditions (Eqs. 7a and 7b) for K_1 and K_4 along with the interchange formula (Eq. 7c) for K_2 and K_3, integrating the first integral in $\delta\Lambda$ from Eq. 26 by parts, and applying the divergence theorem in V_s, we have the first-order expression in the variation:

$$\begin{aligned}
\frac{1}{2} V\delta\Lambda = {} & \chi^2 C \int_\Sigma d^2\underline{r}\,\delta T(\underline{r})\underline{\eta}\cdot\lambda_s\nabla T(\underline{r}) \\
& + \chi^2 C \int_{\Sigma_o+\Sigma_L} d^2\underline{r}\,\delta T(\underline{r})\underline{\eta}\cdot\lambda_s\nabla T(\underline{r}) \\
& - \chi^2 C \int_{V_s} d^3\underline{r}\,\delta T(\underline{r})\nabla\cdot[\lambda_s\nabla T(\underline{r})] \\
& + \chi^2 \frac{\alpha}{1-\alpha}\int_\Sigma d^2\underline{r}\,\delta E_r(\underline{r})[E_r(\underline{r}) - CT(\underline{r})] \\
& - \chi^2 \frac{\alpha}{1-\alpha}\int_\Sigma d^2\underline{r}\,C\delta T(\underline{r})[E_r(\underline{r}) - CT(\underline{r})] \\
& + \chi^2 \int_\Sigma d^2\underline{r}\,\delta E_r(\underline{r})\Bigg[E_r(\underline{r}) \\
& - \int_\Sigma K_1(\underline{r},\underline{r}')E_r(\underline{r}')d^2\underline{r}' \\
& - \int_{V_o} K_2(\underline{r},\underline{r}')E_\phi(\underline{r}')d^3\underline{r}'\Bigg] \\
& + \int_{V_o} d^3\underline{r}\,\delta E_\phi(\underline{r})\Bigg[E_\phi(\underline{r}) \\
& - \int_\Sigma K_3(\underline{r},\underline{r}')E_r(\underline{r}')d^2\underline{r}' \\
& - \int_{V_\phi} K_4(\underline{r},\underline{r}')E_\phi(\underline{r}')d^3\underline{r}'\Bigg]
\end{aligned} \tag{28}$$

Note also, the $K_1 - \chi^2 K_2$ probability sum (Eq. 20) provides a coefficient of one for $E_r(\underline{r})$ in the bracketed integrand term of the second to last integral in Eq. 28, while the $\chi^{-2}K_3 - K_4$ probability Eq. 21 gives a unity coefficient for $E_\phi(\underline{r})$ in the bracketed sum of the last integral of Eq. 28. To see that all first-order terms vanish, the second integral is zero because T^* must satisfy boundary conditions (Eq. 27) such that $\delta T = 0$ on end boundaries. The third integral in Eq. 28 is identically zero by Eq. 16, the first and fifth integrals combine to vanish with Eq. 18, the fourth and sixth integrals cancel because of Eq. 13, and the seventh integral is zero from Eq. 15. From the interpretation of K's as probabilities, the integrals in the variational principle (Eq. 26) and hence $\delta^2\Lambda$ are clearly positive and since all first-order terms in the variation of Λ vanish, that is, $\delta\Lambda = 0$, the variational principle is indeed an upper bound with:

$$\Lambda\{E_r, E_\phi, T_s\} \le \Lambda\{E_r^*, E_\phi^*, T_s^*\}. \tag{29}$$

To relate $\Lambda\{E_r, E_\phi, T\}$ to the heat flux Q, one can start with Eq. 26 in terms of E_r, E_ϕ, and T, and repeat the same steps used to derive Eq. 28, except that the second integral will not be zero. Alternatively, the derived form of Eq. 28 with $2\delta T$, $2\delta E_r$, and $2\delta E_\phi$ replaced, respectively, by T, E_r, and E_ϕ is $\Lambda\{E_r, E_\phi, T\}$, as above all terms vanish except the second integral, and the second integral in $\Lambda\{E_r, E_\phi, T\}$ is just $-\chi^2\underline{Q}\cdot\underline{\beta}$ by Eq. 24. The variational upper bound on the heat flux is, therefore:

$$-\chi^2\underline{Q}\cdot\underline{\beta} = \Lambda\{E_r, E_\phi, T\} \le \Lambda\{E_r^*, E_\phi^*, T^*\}. \tag{30}$$

An effective thermal conductivity λ_e for the slab can be defined as $|Q/\theta|$, and from Eq. 30:

$$C\theta^2\chi^2\lambda_e \le \Lambda\{E_r^*, E_\phi^*, T^*\} \tag{31}$$

If the exact solutions T, E_ϕ, and E_r are substituted into the upper bound, (Eqs. 26-31), then the exact effective conductivity is calculated; otherwise, the result is an upper bound on the effective conductivity.

Trial Functions and Integrations

In this section a variational equation for the pore gas conductivity for a single spherical cavity (Figure 2) will be calculated from the variational principle (Eqs. 26-31) for the effective conductivity of a thick slab of solid phase s surrounding a single spherical void containing a gas phase g. A suitable trial function for the temperature in the solid is suggested by the solution of the thermal conduction problem:

$$T^* = \overline{T} + \underline{\theta}\cdot\underline{R} + \zeta(a/R)^{3-\epsilon}\underline{\theta}\cdot\underline{R} \quad (\underline{R} \text{ in } V_s) \tag{32}$$

where $\overline{T}$ is the average temperature across the void, $\underline{\theta}$ is the temperature difference across the slab, a is the spherical void radius, $\underline{R}$ is a radial vector in the void drawn from its center, and ϵ is a very small positive parameter that guarantees convergence of the variational integrals of Eq. 26 in V_s. ϵ is eventually neglected. When λ_s and $\lambda_g^\dagger$ are the Fourier thermal conductivities, respectively, of the s and g phases, the form of Eq. 32 is exact and the parameter ζ takes the form:

$$\zeta^\dagger = \frac{\lambda_s - \lambda_g^\dagger}{2\lambda_s + \lambda_g^\dagger} \tag{33}$$

However, for arbitrarily low gas pressure in the void, the form of ζ is determined by optimization of the variational integrals. The temperatures in the interface condition (Eq. 18) refer to those of the solid, hence from Eq. 32 substituted into Eq. 18:

$$E_r^*(\underline{r}) = CT^*(\underline{r}) + \omega\underline{\theta}\cdot\underline{\eta}(\underline{r}) \quad (\underline{r} \text{ on } \Sigma). \tag{34}$$

$\underline{\eta}$ is a unit normal on Σ pointing into the void. Rather than imposing a value on ω in terms of ζ from Eqs. 18 and 32, we will allow the optimization of the variational principle to select ω, since for a physically appropriate trial function, this will always give us the correct $\underline{\omega}$ value. The gas temperature in the void is not necessarily continuous with the solid temperature at the void-solid interface. While temperature jump is usually associated with lower pressures (Present, 1958), it can occur even at atmospheric pressures if the thermal accommodation coefficient α is sufficiently small. Within the void, we use the equilibrium conditions (Eq. 23) to relate the trail E_ϕ^* to the trial gas temperature T_g^*. Laplace's equation suggests a linear temperature profile in the gas void space and:

$$E_\phi^* = \chi^2 C T_g^* = \chi^2 C[\overline{T} + \nu(1+\zeta)\underline{\theta}\cdot\underline{R}] \quad (\underline{R} \text{ in } V_\phi) \tag{35}$$

but unlike the T^* from Eq. 32 the variationally optimized parameter ν in Eq. 35 will account for temperature jump and should range in value from zero to one.

When the trial functions (Eqs. 32, 34, and 35) are substituted into the variational principle (Eq. 26), five types of integrals are found. Owing to the simple geometry of the spherical void and the appropriateness of the trial functions, the evaluation of these integrals is straightforward. The single solid and surface integration, the first two integrals listed in Eq. 26, are easily performed and substituting these results into Eqs. 26 and 31 yields the expression:

$$\begin{aligned}\lambda_e \le \lambda_s[(1-\phi) - 2\zeta\phi + 2\zeta^2\phi] + Ca\phi\alpha(1-\alpha)^{-1}\mu^2 \\ + Ca\phi[(1+\zeta)^2(\sigma_1 - 2\nu\sigma_2 + \nu^2\sigma_3) \\ - 2(1+\zeta)\mu(\sigma_1 - \nu\sigma_2) + \mu^2\sigma_1]\end{aligned} \tag{36}$$

where $\mu = \omega(aC)^{-1}$ and ϕ is the void to total volume ratio. Note to equate the three σ_1 integral forms that appear in Eq. 36, the vector relation $\underline{R} = -a\underline{\eta}(\underline{r})$ must be used in the K_1 double surface integrals.The forms of σ_1, σ_2, and σ_3, and the values for a spherical void are given in terms of the Knudsen number:

$$Kn = \ell/(2a) \tag{37}$$

as

$$\begin{aligned}\sigma_1 = \frac{1}{2a\phi\theta^2}\int_\Sigma d^2\underline{r}\int_\Sigma d^2\underline{r}\,' K_1(\underline{r},\underline{r}\,')(\underline{\theta}\cdot\underline{\rho})^2 \\ + \frac{\chi^2 a}{\phi\theta^2}\int_\Sigma d^2\underline{r}\int_{V_\phi} d^3\underline{r}\,' K_2(\underline{r},\underline{r}\,')[\underline{\theta}\cdot\underline{\eta}(\underline{r})]^2\end{aligned} \tag{38}$$

$$\begin{aligned}= 1 - 2Kn^2 + 24Kn^4 - 2Kn\exp(-Kn^{-1}) \\ [1 + 5Kn + 12Kn^2 + 12Kn^3]\end{aligned} \tag{39}$$

$$\sigma_2 = \frac{\chi^2}{\phi\theta^2}\int_\Sigma d^2\underline{r}\int_{V_\phi} d^3\underline{r}\,' K_2(\underline{r},\underline{r}\,')[\underline{\theta}\cdot\underline{\eta}(\underline{r})][a\underline{\theta}\cdot\underline{\eta}(\underline{r}) - \underline{\theta}\cdot\underline{\rho}] \tag{40}$$

$$\begin{aligned}= 1 - (4Kn/3) - 2Kn^2 + 32Kn^4 - 2Kn\exp(-Kn^{-1}) \\ \times[1 + 7Kn + 16Kn^2 + 16Kn^3]\end{aligned} \tag{41}$$

and

$$\begin{aligned}\sigma_3 = \frac{\chi^2}{a\phi\theta^2}\int_\Sigma d^2\underline{r}\int_{V_\phi} d^3\underline{r}\,' K_2(\underline{r},\underline{r}\,')[\underline{\theta}\cdot\underline{\rho} - a\underline{\theta}\cdot\underline{\eta}(\underline{r})]^2 \\ + \frac{\chi^2}{2a\phi\theta^2}\int_{V_\phi} d^3\underline{r}\int_{V_\phi} d^3\underline{r}\,' K_4(\underline{r},\underline{r}\,')(\underline{\theta}\cdot\underline{\rho})^2\end{aligned} \tag{42}$$

$$\begin{aligned}= 1 - 6Kn^2 + 48Kn^4 - 2Kn\exp(-Kn^{-1}) \\ \times[1 + 9Kn + 24Kn^2 + 24Kn^3].\end{aligned} \tag{43}$$

It is of some interest to examine the structure of the variational solution. In terms of the various σ functions (Eqs. 38-43) and the thermal accommodation α, a quantity λ_g with the units of thermal conductivity is defined:

$$aC\lambda_g^{-1} = \sigma_3(\sigma_1\sigma_3 - \sigma_2^2)^{-1} + (1-\alpha)\alpha^{-1} \tag{44}$$

When the variational principle (Eq. 36) is successively minimized with respect to μ, ν, and ζ, and the three extremum equations are simultaneously evaluated for their optimum values μ_o, ν_o, and ζ_o, we obtain:

$$\mu_o = \frac{\omega_o}{aC} = \frac{(1-\alpha)}{\alpha}\frac{\lambda_g}{aC}\left(\frac{3\lambda_s}{2\lambda_s + \lambda_g}\right) \tag{45}$$

or alternatively,

$$\omega_o = [(1-\alpha)/\alpha]\lambda_s(1 - 2\zeta_o) \tag{46}$$

after substituting into Eq. 45 the minimizing value of ζ,

$$\zeta_o = (\lambda_s - \lambda_g)(2\lambda_s + \lambda_g)^{-1} \tag{33}$$

We find as well:

$$(\nu_o)^{-1} = \sigma_3\sigma_2^{-1} + (1-\alpha)\alpha^{-1}(\sigma_1\sigma_3 - \sigma_2^2)\sigma_2^{-1} \tag{47}$$

and finally the slab conductivity:

$$\lambda_e \le \lambda_s[1 - 3\phi(\lambda_s - \lambda_g)(2\lambda_s + \lambda_g)^{-1}]. \tag{48}$$

Equation 46 gives the extremum value of the parameter ω, introduced in the trial function (Eq. 34) for $E_r^* - CT_s^*$. If this trial function (Eq. 34) had been inserted into the interface transport equation (Eq. 18) along with the trial function (Eq. 32) for T_s^*, the parameter ω would have been specified in terms of α, λ_s, and ζ. In a variational calculation it is usually always better to leave a parameter free to vary, because if the trial functions are not exact, the parameter will select its best optimizing value. But in this case both the variational optimization of Eq. 36 and the interface transport Eq. 18 give the

same optimum form (Eq. 46) of ω. The form (Eq. 33) of ζ_o has already been identified, earlier in the article, as the exact form of ζ for the thermal profile of a spherical void of conductivity λ_g encased in a large slab of conductivity λ_s. The variational upper bound expression (Eq. 48) for the net slab-void conductivity λ_e can also be shown to be the correct form of λ_e for a single sphere in a large slab (Devera and Strieder, 1977). The parameters and net thermal conductivity are the appropriate forms of Maxwell's solution of the single sphere problem, provided we identify λ_g from Eq. 44 with the void gas thermal conductivity. Indeed in cryogenic design (Kaganer, 1969), one usually derives a Knudsen-transition-bulk void gas thermal conductivity λ_g; then in the modeling equations for the insulation, treats the gas phase as a simple Fourier conductor. The gas conductivity (Eq. 44) for λ_g is precisely that expression for a spherical cavity.

In the context of the cryogenic insulation equations, the λ_g form (Eq. 44) will appropriately include any temperature jump at the void-solid interface in the insulation conductivity at an arbitrary gas pressure. The variational parameter ν from the gas-phase trial temperature (Eq. 35) is a direct measure of void-solid interface temperature jump for a spherical cavity, that is for a continuous temperature at the interface $\nu = 1$ and for the most severe jump with no thermal gradient in the sphere $\nu = 0$. The optimum value ν_o of the parameter (Eq. 47) from Eqs. 39, 41, and 43 is shown in Figure 3 plotted vs. the inverse Knudsen number Kn^{-1} for various values of the thermal accommodation coefficient α from 1 to 0.01. Knudsen and bulk plateaus are evident for any α and at low gas pressure, high Knudsen numbers, a significant interfacial temperature jump ($\nu_o < 1$) is seen to occur at any α, decreasing to the extreme case of no void gradient at $\alpha = 0$. Usually inverse Knudsen numbers near 10^3 are associated with normal atmospheric pressures. Customarily α is ignored and the handbook bulk gas and solid conductivities are combined with an assumption of

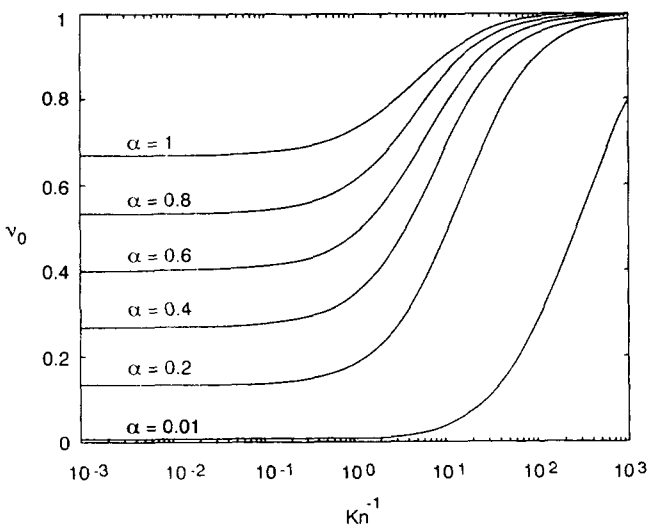

Figure 3. Void gas temperature-jump parameter ν_o for spherical cavity vs. inverse Knudsen number Kn^{-1} ($=2a/\ell$) for thermal accommodation coefficients.

$\nu_o = 1$ gives a continuous gas to solid at the cavity surface, while, $\nu_o = 0$ corresponds to the most severe temperature jump (void gas gradient vanishes).

a continuous interfacial temperature in the transport calculation. In Fig. 3 at the higher-pressure, large inverse Knudsen number, side for most α values ν is nearly unity, however, the curves indicate that for α below 0.1, significant temperature jump can occur even at atmospheric pressure and above. Values of α this small have been recorded (Saxena and Joshi, 1981) and the standard gas conductivity table will give no warning of these difficulties.

The variational expression λ_g from Eq. 44, with Eqs. 39, 41, and 43 for σ_1, σ_2, and σ_3, provides a rigorous analytical upper bound on the void gas conductivity as a function of the Knudsen number. Note that a plot of λ_e vs. increasing λ_s for fixed $\overline{T}$, $\overline{P}$, and α should exhibit a single cross over from above to below the 45° diagonal line at the point $\lambda^{\dagger}_s = \lambda^{\dagger}_e = \lambda^{\dagger}_g$. Applying the inequality (Eq. 48) at this point gives the expression (Eq. 44) for λ_g as a rigorous upper bound on $\lambda^{\dagger}_s$ and hence the true void gas conductivity $\lambda^{\dagger}_g$. In the low pressure, large Knudsen number limit, the trial temperature form (Eq. 32) is the correct temperature profile and

$$\lim_{Kn\to\infty} \lambda_g = \lambda_{Kn} = \alpha Ca \tag{49}$$

is the exact void conductivity as found by Tsia and Strieder (1985) for a spherical cavity. This result differs from the parallel plate Knudsen thermal conductivity (Eq. 2) in the accommodation coefficient dependence. The $\alpha(2-\alpha)^{-1}$ multiplier of Eq. 2 is replaced by α. While both equations are solutions to Knudsen heat transport, Eq. 49 represents the Knudsen conductivity with a more realistic pore geometry for a closed cell media (spherical void) than that of infinite parallel plates. In the opposite bulk pressure, low Knudsen number limit where α is not small, again the trial temperature functions in the void (Eq. 35) and solid (Eq. 32) are exact forms and from Eqs. 14 and 37, we have:

$$\lim_{Kn\to o} \lambda_g = \lambda_o = \frac{\ell}{6}\left(\frac{\gamma+1}{\gamma-1}\right) nk\bar{v} \tag{50}$$

where ℓ is the mean free path and γ is the heat capacity ratio. In general, λ_o is neither a function of pressure or pore spacing in the bulk limit, and like the Knudsen limit of Eq. 44 is also an exact solution. For a monatomic gas ($\gamma = 5/3$) Eq. 50 predicts a mean free path bulk gas thermal conductivity:

$$\lambda_o = 2\ell n\bar{v}k/3 \quad \text{(monatomic gas)} \tag{51}$$

which contrasts with the simple kinetic theory (SKT) bulk gas conductivity

$$\lambda_o(SKT) = \ell n\bar{v}k/2 \quad \text{(monatomic gas)} \tag{52}$$

found in Bird et al. (1960). The bulk conductivity (Eqs. 50 and 51) contains a correction to the SKT value (Eq. 52) to account for the swifter molecules, which are more likely to transport energy. For example for a plane drawn across a gas the average energy of a gas molecule crossing the surface from above to below is not $3kT/2$ as assumed by SKT, but must be $2kT$ (Kestin and Dorfmann, 1971). In a given direction and fixed time interval, the faster molecules with higher speed and

kinetic energy will preferentially cross a planar surface, whereas the slower molecules may not make it at all. This requires that the SKT conductivity (Eq. 52) be increased by a factor of 4/3, which produces the improved result (Eq. 51). If $2kT$ is not used, the physical transport model will not satisfy the equilibrium limit, for it is well known for an arbitrary plane drawn through a gas in Maxwellian equilibrium, the average energy of a monatomic gas molecule crossing the plane in either direction has to be $2kT$. Further, $2kT$ will agree with detailed balancing at the gas surface interface.

In between the limits Springer (1971), Kaganer (1969), and many others have used the series additivity interpolation formula (Eq. 1) for the void gas conductivity, and it would be useful to compare this form against the variational void gas conductivity (Eq. 44). In Figure 1, the thermal conductivity ratio $\lambda_g^{-1}(\lambda_o^{-1}+\lambda_{Kn}^{-1})^{-1}$, using Eq. 44 for all three conductivity forms, is given vs. the inverse Knudsen number for various thermal accommodation coefficients from 0.01 to 1. Of course in the limits of large and small Kn^{-1} a ratio of unity is obtained. For smaller α the series equation works well at any gas pressure. At higher accommodation, an absolute minimum deviation of λ_g (series) λ_g^{-1} of 5-6% at $\alpha=1$ and $Kn\approx 1/2$, is still reasonable agreement. The minima in Figure 1 lie slightly toward the lower Knudsen number side and tend to shift further in this direction, but decrease in magnitude, as thermal accommodation decreases over the physical range of α values from 1 to 0.01.

The solid lines in Figures 4a and 4b, which give the dimensionless gas-phase conductivity λ_g/λ_o vs. the inverse Knudsen number Kn^{-1} from Eqs. 44 and 50, generate the familiar S curves for various thermal accommodation coefficients α. In practice α values near unity do occur, and α is rarely below 0.01, so for a spherical void the range of possible λ_g/λ_o values lies between the extreme right- and left-solid curves. The solid line S curves have two plateaus, a Knudsen plateau below $Kn^{-1}=10^{-3}$ and the bulk, continuum plateau of unity at higher above $Kn^{-1}=10^{3}$. Between these plateaus, the gas conductivity drops significantly with decrease in Kn^{-1} (drop in pressure). For $\alpha<0.1$ the consequence of the bulk plateau shift to higher Kn^{-1} (larger pressures) has already been discussed in Figure 3 and related to the presence of temperature jump.

Harper and El Sahrigi (1964) have measured the effective thermal conductivity of a polyurethane foam using a series of void gases, H_2, He, Ne, N_2, CO_2 and Freon 12 with increasing molecular weight, respectively, 2, 4, 20, 28, 44, and 121. The foam conductivities for each void gas were determined over a pressure range from atmosphere to 0.005 mm Hg and at a constant average temperature of 35°C. They recorded a foam void fraction ϕ as 0.85 and a pore diameter range of 200-600 microns, from which we will use the midpoint value. The thermal conductivity of the solid plastic polyurethane ($\lambda_s=0.095$ W/mK) was measured in situ during the experiments. The data is interesting because for a single characterized foam and at a fixed average temperature the overall conductivity for various void gases with increasing molecular weight provide a means to study molecular mass m effects on α.

Russel's equation has been recommended and used by Kaganer (1969) for cellular foam materials in his monograph on cryogenic insulation to calculate λ_{eff} given λ_s, λ_g, and ϕ:

$$\lambda_{eff}=\lambda_s\frac{\phi^{2/3}+(\lambda_s/\lambda_g^{\dagger})(1-\phi^{2/3})}{\phi^{2/3}-\phi+(\lambda_s/\lambda_g^{\dagger})(1-\phi^{2/3}+\phi)}. \tag{53}$$

It is reasonable given ϕ, λ_s, and λ_{eff} to use the same equation to back out λ_g, which provides from Harper and El Sahrigi's data (1964) void gas conductivity pressure curves for the various gases. The pressure values $\overline{P}$ for the various gases are converted to inverse Knudsen numbers to standardize the curves for comparison by:

$$Kn^{-1}=\frac{a}{3\lambda_o}\left(\frac{\gamma+1}{\gamma-1}\right)\frac{\overline{P}\overline{v}}{\overline{T}} \tag{54}$$

where gas bulk conductivity λ_o values and heat capacities

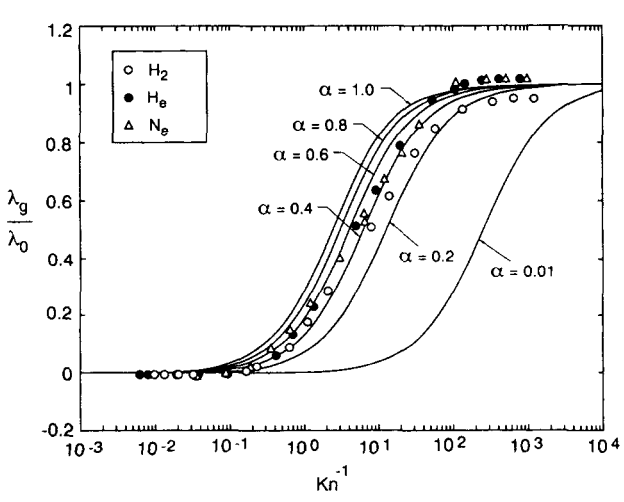

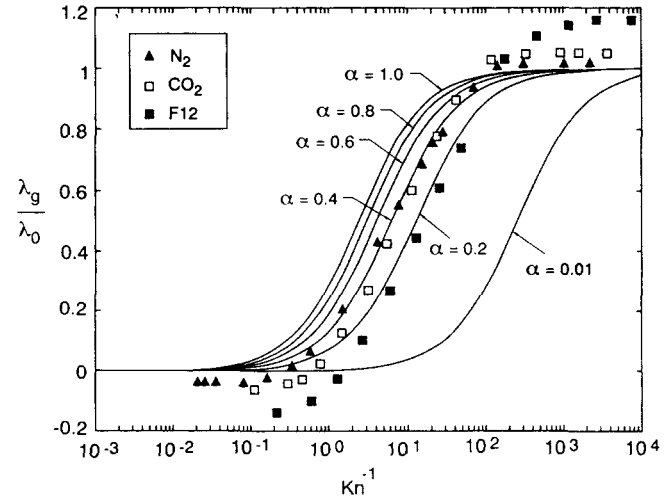

Figure 4. Dimensionless void gas thermal conductivity (λ_g/λ_o) vs. dimensionless gas pressure (Kn^{-1}).
S curves for various thermal accommodation coefficients are from mean free path theory, Eq. 44. Various points refer to experimental conductivities (Harper and El Sahrigi, 1964) for gases with increasing molecular weight. Lighter gases, H_2 (2), He (4), and Ne (20), in Figure 4a show an increasing trend in α with molecular weight, and the heavier gases in Figure 4b, N_2 (28), CO_2 (44), F-12 (121), display the decrease in α with increasing molecular weight, which starts with Ne. Experimental results suggest a maximum α value between He and Ne.

are readily available and the mean thermal speed $\bar{v}$ $[=\sqrt{8k\bar{T}/(\pi m)}]$. Since the data points overlap, the S curves are split into the lighter H_2, He, and Ne in Figure 4a and the heavier gases N_2, CO_2, and Freon 12 in Figure 4b. The experimental bulk gas conductivities on the right side of Figure 4a show that Russel's equation works very well for light molecules. That the gas bulk conductivities of the heavier CO_2 and Freon 12 lie above one in Figure 4b is consistent with their higher λ_s/λ_o ratio values, respectively, 5.6 and 9.2. At lower Knudsen gas pressures, and even larger λ_s/λ_g ratios, the difficulties with Russel's equation appear to be symmetric.

The shape of the experimental λ_g/λ_o curves in Figures 4a and 4b are qualitatively similar to the variational S curves as expected. These experimental points were calculated from λ_{eff} vs. pressure data using no adjustable constants. While the cell diameter is approximate and the actual foam cells are not identical spheres, the experimental λ_g/λ_o curves always lie to the left of the $\alpha=1$ curve and to the right of the curve for $\alpha=0.01$ predicted by mean free path theory. The experimental data points in Figure 4a suggest a thermal accommodation coefficient for H_2 on polyurethane of about 0.4. Accommodation seems to increase from the H_2 values to about 0.7 for the heavier molecules He and Ne. Then, in Figure 4b with increasing molecular mass N_2, CO_2, and F-12 show a decreasing trend from $\alpha=0.4$ for H_2 down to a minimum α value of just under 0.2 for F-12. That a maximum appears between He of molecular weight 4 and Ne with molecular weight 20, in the range of the dominant atomic species on the polyurethane surface, seems to agree with those molecular theories for α that have their origins in Baule's molecular collision theory (Saxena and Joshi, 1981).

Summary and Conclusions

In this article, mean free path gas kinetic theory was used to model the conductive heat transport of a gas within a void volume enclosed in a Fourier solid as a function of pressure. A variational upper bound principle on the thermal conductivity of a slab containing a void of arbitrary shape was derived. A variational upper bound for the gas conductivity in a spherical void valid from the Knudsen to the continuum limit was calculated. The following results and conclusions were obtained:

(1) The trial function optimization produced a temperature jump coefficient equation. We found that temperature jump will occur either at low pressure for any thermal accommodation coefficient or for a small α ($\alpha<0.1$) even at atmospheric pressure and above (Figure 3).

(2) A rigorous upper bound variational equation for the void gas conductivity valid from the Knudsen to the continuum limit was derived for a spherical void. The equation was shown to be exact in both the large and small Knudsen number limit. The validity of a correction factor of 4/3 for the simple mean free path bulk thermal conductivity was established.

(3) The reciprocal additivity interpolation formula was demonstrated to be a reasonable approximation in the spherical void, gas thermal conductivity problem. (It had been justified previously only in the mass-transfer problem.) Reciprocal additivity is very accurate for smaller thermal accommodation coefficients, but does give a measurable error (6%) for higher α and $0.1<Kn<10$ (Figure 1).

(4) Experimental heat conductivity vs. pressure data (Harper and El Sahrigi, 1964) were converted to dimensionless, standardized forms of the void gas to bulk thermal conductivity ratio vs. inverse Knudsen number curves, and compared with good agreement to mean free path theory S curves from Eq. 44 drawn for various α in the range $0.01<\alpha<1$. That thermal accommodation coefficients for polyurethane surfaces at 35°C start for H_2 roughly at 0.4, go through a maximum somewhere between He and Ne of about 0.7, then decrease with increasing molecular weight down to below 0.2 for F-12 (Figures 4a and 4b), agrees qualitatively with the maximum in α with the masses of the gas predicted by Baule's theory (Kennard, 1938; Saxena and Joshi, 1981). The results in Figure 4 show that the shift in the S curve with the thermal accommodation coefficient α will enhance the insulating ability for the heavier molecules, and in some instances a small $\alpha<0.01$ for a lighter gas might even balance the higher thermal conductivity.

Acknowledgment

Acknowledgment is made to the Donors of the Petroleum Research Fund, administered by the American Chemical Society, for support of this research.

Notation

a = sphere radius
c_v = constant volume heat capacity
c_p = constant pressure heat capacity
C = defined in Eq. 14
$d^2\underline{r}$ = differential element of surface
$d^3\underline{r}$ = differential element of volume
E_i = energy flux of gas molecules incident to surface
E_r, E_r^* = energy flux and energy flux trial function of gas molecules leaving surface
E_w = energy flux of gas molecules in equilibrium with the surface leaving surface
E_ϕ, E_ϕ^* = total energy of the gas molecules that undergo a molecule-molecule collision within a unit volume at $\underline{r}$ and are emitted from that volume per unit time and trial function
$\underline{i}$ = unit vector across the slab in the direction from $x=0$ to $x=L$
k = Boltzmann constant
Kn = Knudsen number, $=\ell/2a$
$K_1(\underline{r}, \underline{r}')$, $K_2(\underline{r}, \underline{r}')$, $K_3(\underline{r}, \underline{r}')$, $K_4(\underline{r}, \underline{r}')$ = free path probabilities surface collision at $\underline{r}$ to surface collision at $\underline{r}'$, void molecular collision at $\underline{r}$ to surface collision at $\underline{r}'$, surface collision at $\underline{r}$ to void collision at $\underline{r}'$ and void molecular collision at $\underline{r}$ to void collision at $\underline{r}$, given by Eqs. 3-6
ℓ = mean free path of gas molecules
L = slab thickness
$\underline{n}$ = particle (molecule) number density
P = average pressure of the gas in the void
$\underline{Q}$ = net heat flux across plane of slab in x direction per unit total cross section
$\underline{r}$, $\underline{r}'$ = location vectors in the slab
$\underline{R}$ = radial vector pointing away from the center of a sphere
T_g^* = trial temperature of gas phase
T_o, T_L = constant temperatures at $x=0$ and $x=L$
T = average temperature $(T_L+T_0)/2$ and surface average temperature of spherical void
T_w = temperature of wall
$\bar{v}$ = mean thermal speed
V = total volume of the slab
V_s = total solid volume
V_ϕ = total void volume
x = coordinate running from 0 to L across slab

Greek letters

α = accommodation coefficient
$\underline{\beta}$ = defined by Eq. 25
γ = heat capacity ratio, c_p/c_v
δ = distance dimension in Eq. 2
δT, δE_r, δE_ϕ = variations in T, E_r, and E_ϕ
ζ, ζ_0 = variational parameter in Eq. 32 and optimum value
$\underline{\eta}$ = unit surface normal pointing away from the solid
$\underline{\theta}$ = temperature gradient defined by Eq. 25
λ_e = effective conductivity
$\lambda_g^\dagger$ = true spherical pore gas conductivity
λ_g = upper bound on void gas conductivity, Eq. 44
λ_{Kn} = Knudsen gas conductivity
λ_o = continuum gas conductivity
λ_s = solid conductivity
Λ = defined by Eq. 26
μ, μ_o = variational parameter introduced in Eq. 36 and optimum value
ν, ν_o = variational parameter in Eq. 35 and optimum value
$\underline{\rho}$ = $=\underline{r}' - \underline{r}$, relative position vector
σ_1, σ_2, σ_3 = defined in Eqs. 38, 40,and 42
Σ = void-solid interface
Σ_o, Σ_L = planer surfaces located at $x=0$ and $x=L$, respectively
ϕ = void fraction or sphere void to total slab volume ratio
χ = defined by Eq. 8
ψ = $=n\bar{v}/4$ or $P(2\pi mkT)^{1/2}$, effusive mass driving force
ω, ω_o = variational parameter in Eq. 34 and optimum value

Literature Cited

Barron, R. F., *Cryogenic Systems*, Clarendon Press, Oxford, p. 383 (1985).

Bird, R. B., W. E. Stewart, and E. N. Lightfoot, *Transport Phenomena*, Wiley, New York, p. 255 (1960).

Boetes, R., and C. J. Hoogendorn, "Heat Transfer in Polyurethane Foams for Cold Insulation," *Heat and Mass Transfer in Refrigeration and Cryogenics*, J. Bougard and N. Afgan, eds., Hemisphere, Washington, DC, p. 14 (1987).

Chambré, P., "On Chemical Reactions in Free Molecule Flow," *J. Chem. Phys.*, **32**, 24 (1960).

Clausing, P., "Over den verblijtijd van moleculen en de strooming van zeer verdunde gassen," PhD Thesis, Leyden (1929).

Cunningham, G. R., Jr., and C. L. Tien, "Heat Transfer in Microsphere Insulation in the Presence of a Gas," *15th International Conference on Thermal Conductivity*, Plenum Press, New York, pp. 325-333 (1977).

Devera, A. L., and W. Strieder, "Upper and Lower Bounds on the Thermal Conductivity of a Random, Two-Phase Medium," *J. Chem. Phys.*, **81**, 1783 (1977).

Hands, B. A., "A Survey of Cryogenic Engineering," *Cryogenic Engineering*, B. A. Hands, ed., Academic Press, New York, p. 1 (1986).

Harper, J. C., and A. F. El Sahrigi, "Thermal Conductivities of Gas Filled Porous Solids," *I. and E. C. Fund*, **3**, 318 (1964).

Ho, G. F., and W. Strieder, "Numerical Evaluation of the Porous Medium Effective Diffusivity between the Knudsen and Continuum Limits," *J. Chem. Phys.*, **73**, 6296 (1980).

Kaganer, M. G., *Thermal Insulation in Cryogenic Engineering*, Israel Program of Scientific Translations Ltd., Jerusalem (1969).

Kennard, E. H., *Kinetic Theory of Gases*, McGraw-Hill, New York, pp. 311-325 (1938).

Kestin, J., and J. R. Dorfman, *A Course in Statistical Thermodynamics*, Academic Press, New York, p. 521 (1971).

Kramer, J.-J., E. W. Brogren, and G. L. Siegel, "Evaluation of Propellant Tank Insulation for Low Thrust Chemical Propulsion Systems," NASA Report No. NASA CR-168320 (1984).

Pleasant, R. L., "Heat Transfer through Liquid Hydrogen Tank Insulation of Shuttle/Center G-Prime," *Cryogenic Properties, Processes and Applications*, A. J. Kidnay, J. J. Hiza, T. M. K. Frederking, P. J. Kerney and L. A. Wenzel, eds., AIChE Symp. Ser., Vol. 82, p. 75 (1986).

Pollard, W. G., and R. D. Present, "On Gaseous Self-Diffusion through Long Capillary Tubes," *Phys. Rev.*, **73**, 762 (1948).

Present, R. D., *Kinetic Theory of Gases*, McGraw-Hill, New York, p. 33 (1958).

Saxena, S. C., and R. K. Joshi, *Thermal Accommodation and Adsorption Coefficients of Gases*, Vol. II-1, McGraw-Hill, New York (1981).

Shidlovskiy, V. P., *Introduction to Dynamics of Rarefied Gases*, Elsevier, New York (1967).

Springer, G. S., "Heat Transfer in Rarefied Gases," *Advances in Heat Transfer*, J. P. Harnett and T. F. Irvine, eds., Vol. 7, Academic Press, New York, p. 163 (1971).

Strieder, W. C., "Gaseous Self-Diffusion through a Porous Medium," *J. Chem. Phys.*, **54**, 4050 (1971).

Tien, C. L., and A. J. Streton, "Heat Transfer in Low Temperature Insulations," *Heat and Mass Transfer in Refrigeration and Cryogenics*, J. Bougard and N. Afgan, eds., Hemisphere, Washington, DC, p. 3 (1987).

Timmerhaus, K. D., "Conductive Heat Transfer," *Heat Transfer at Low Temperatures*, W. Frost, ed., Plenum Press, New York, p. 9 (1975).

Tsai, D-S., and W. Strieder, "Radiation across a Spherical Cavity having Both Specular and Diffuse Reflectance Components," *Chem. Eng. Sci.*, **40**, 170 (1985).

Wakao, N., and D. Vortmeyer, "Pressure Dependency of Effective Thermal Conductivity of Packed Beds," *Chem. Eng. Sci.*, **26**, 1753 (1971).

Zheng, L., and W. Strieder, "Knudsen Void Gas Heat Transport in Fibrous Media," *Int. J. Heat Mass Transport*, **37**, 1433 (1994).

Manuscript received July 23, 1993, and revision received Oct. 12, 1993.